The Cell Surface 7 (2021) 100057

Contents lists available at ScienceDirect

The Cell Surface

journal homepage: www.sciencedirect.com/journal/the-cell-surface

Inactivating the mannose-ethanolamine phosphotransferase Gpi7 confers caspofungin resistance in the human fungal pathogen *Candida albicans*

Guisheng Zeng [a], Xiaoli Xu [a], Jiaxin Gao [a], Alessandra da Silva Dantas [b], Neil A.R. Gow [b], Yue Wang [a,c,*]

[a] Institute of Molecular and Cell Biology, 61 Biopolis Drive, Proteos, Singapore 138673, Singapore
[b] MRC Centre for Medical Mycology, School of Biosciences, University of Exeter, Stocker Road, Exeter EX4 4QD, UK
[c] Department of Biochemistry, Yong Loo Lin School of Medicine, National University of Singapore, Singapore 117597, Singapore

ARTICLE INFO

Keywords:
Fungal pathogens
Antifungal resistance
Caspofungin
Cell wall
Chitin synthesis

ABSTRACT

Understanding the molecular mechanisms governing antifungal resistance is crucial for identifying new cellular targets for developing new antifungal therapeutics. In this study, we performed a transposon-mediated genome-wide genetic screen in haploid *Candida albicans* to identify mutants resistant to caspofungin, the first member of the echinocandin class of antifungal drugs. A mutant exhibiting the highest resistance possessed a transposon insertion that inactivates *GPI7*, a gene encoding the mannose-ethanolamine phosphotransferase. Deleting *GPI7* in diploid *C. albicans* caused similar caspofungin resistance. *gpi7*Δ/Δ cells showed significantly elevated cell wall chitin content and enhanced phosphorylation of Mkc1, a core component of the PKC-MAPK cell-wall integrity pathway. Deleting *MKC1* suppressed the chitin elevation and caspofungin resistance of *gpi7*Δ/Δ cells, but overexpressing the dominant inactive form of *RHO1*, an upstream activator of PKC-MAPK signaling, did not. Transcriptome analysis uncovered 406 differentially expressed genes in *gpi7*Δ/Δ cells, many related to cell wall construction. Our results suggest that *GPI7* deletion impairs cell wall integrity, which triggers the cell-wall salvage mechanism via the PKC-MAPK pathway independently of Rho1, resulting in the compensatory chitin synthesis to confer caspofungin resistance.

Introduction

Due to their wide distribution and high incidence worldwide, infectious diseases caused by fungal pathogens are among today's most critical medical problems. *Candida albicans* is one of the most prevalent opportunistic fungal pathogens of humans (Hallen-Adams and Suhr, 2017). On the one hand, *C. albicans* is a member of the natural microflora of the skin, gastrointestinal tract, and genital mucosa in 50–70% of the human population without causing any symptoms (Pfaller and Diekema, 2007). On the other hand, *C. albicans* is the leading cause of hospital-acquired bloodstream infections in immunocompromised patients with high morbidity and mortality rates (Cleveland et al., 2012). Systemic candidiasis is considered one of the most severe fungal infections (Brown et al., 2012), posing a significant public health threat.

Drugs currently available for treating fungal infections are classified into five groups according to their mechanism of action (MOA) (Gizińska et al., 2019). The first group is azoles, such as fluconazole, which inhibit ergosterol synthesis by blocking lanosterol demethylase activity. The second group is polyenes, such as amphotericin B, that bind to ergosterol and impair cell membrane function. The third group is echinocandins, represented by caspofungin, which disrupt cell wall biosynthesis by inhibiting the β-1,3-glucan synthase. Fluorinated pyrimidine derivatives belong to the fourth -group that blocks nucleic acid synthesis. The last group includes allylamines that inhibit squalene epoxidase, causing the intracellular accumulation of toxic substances leading to rapid cell death. Among these five classes of antifungal agents, only azoles, polyenes, and echinocandins are applicable for treating systemic infections (Gizińska et al., 2019).

The limited variety of available antifungal agents and their widespread overuse in prevention and therapy have contributed to the emergence of drug resistance in fungal pathogens worldwide (Aslam et al., 2018). Alarmingly, *Candida* strains resistant to more than one class of antifungals are now often isolated, which threatens to make our entire antifungal drug arsenal obsolete (Fairlamb et al., 2016). So far, several mechanisms of resistance to antifungals have been identified. They include the alteration of drug affinity via mutations on target

* Corresponding author.
E-mail address: mcbwangy@imcb.a-star.edu.sg (Y. Wang).

https://doi.org/10.1016/j.tcsw.2021.100057
Received 26 April 2021; Received in revised form 14 June 2021; Accepted 18 June 2021
Available online 23 June 2021

enzymes, increase of target protein abundance, up-regulation of efflux pumps to reduce intracellular drug levels, biofilm formation, and activation of cellular stress responses (Cowen et al., 2015; Revie et al., 2018; Sanglard, 2016; Vandeputte et al., 2012).

Fungal cells are surrounded by the cell wall that is essential for their viability. The cell wall is a dynamic structure, and its composition and structural organization are regulated during the cell cycle and in response to changing environmental conditions (Klis et al., 2006; Ruiz-Herrera et al., 2006). *C. albicans* cell wall is mainly composed of β-1,3-glucan, β-1,6-glucan, chitin, and cell wall proteins (CWPs), with β-glucans as the main constituents, accounting for 50–60% of the cell wall by weight (Kapteyn et al., 2000; Shepherd, 1987). Together with chitin, the glucans form a rigid skeleton that determines the cell shape and physical strength (Gow et al., 2017; Lenardon et al., 2020; Shepherd, 1987). CWPs are covalently linked to skeletal polysaccharides. Most of these CWPs in *C. albicans* are anchored to the cell wall by a glycosylphosphatidylinositol (GPI) through the linkage to β-1,6-glucan (Chaffin, 2008; Richard and Plaine, 2007). Aside from determining cell shape, the cell wall functions as a permeability barrier and preserves the cell's osmotic integrity by counteracting the high, outward turgor pressure (Klis et al., 2002). Thus, an impaired or damaged cell wall can severely threaten cell survival. Because of its essentiality and absence in mammalian cells, the cell wall has always been an attractive target for developing antifungal agents (Odds et al., 2003).

Caspofungin is the first member of the echinocandin class of antifungal drugs. It blocks β-1,3-glucan biosynthesis by non-competitive inhibition of β-1,3-glucan synthase, causing fibril dysfunction and damage to cell wall integrity (Revie et al., 2018). Since its first use in antifungal treatment in 2001, clinical resistance of *C. albicans* to caspofungin has remained uncommon, although case reports of resistance are increasing (Sanglard, 2016). The most prevalent caspofungin resistance mechanism is mutations in *FKS1,* a gene encoding the catalytic subunit of β-1,3-glucan synthase, the drug target (Balashov et al., 2006; Park et al., 2005). *FKS1* mutations are associated with enhanced expression of chitin synthesis genes, elevating chitin accumulation in the cell wall (Imtiaz et al., 2012; Walker et al., 2013). A large body of evidence intimately links caspofungin resistance to the cell wall salvage mechanism, which increases chitin synthesis to compensate for the loss of cell wall glucan due to echinocandin exposure. The increased chitin content fortifies the cell wall (Walker et al., 2010). Several cellular stress response pathways govern the cell wall salvage mechanism, including protein kinase C (PKC) cell wall integrity and high osmolarity glycerol (HOG) MAP kinase cascades, and Ca^{2+}/calcineurin signaling, which activates compensatory up-regulation of chitin synthesis (Lee et al., 2018; Munro et al., 2007; Walker et al., 2008). In contrast to azoles, resistance to echinocandins is largely unaffected by multidrug transporters (Niimi et al., 2006). Recent studies revealed that multiple genomic alterations are also associated with caspofungin tolerance, such as segmental or chromosomal aneuploidies (Yang et al., 2017). Despite considerable advances, there are drug resistance mechanisms in fungal pathogens remaining unexplained.

In this study, we conducted a transposon-mediated genome-wide genetic screen in haploid *C. albicans* and isolated > 20 transposon-insertional mutants exhibiting caspofungin resistance. One mutant contained an insertional mutation in *GPI7*. Deleting *GPI7* conferred caspofungin resistance, which is associated with increased cell wall chitin content and enhanced phosphorylation of Mkc1, a core component of the PKC-MAPK pathway known to regulate cell wall integrity. Deleting *MKC1* suppressed the chitin elevation and caspofungin resistance of the *gpi*7Δ/Δ mutant while overexpressing the dominant inactive form of Rho1, an upstream Mkc1 activator, did not. *GPI7* deletion also caused the up-regulation of many genes involved in cell wall construction and attenuated *C. albicans* virulence. Our studies suggest that *GPI7* deletion causes cell wall integrity damage, which, in turn, triggers the cell wall salvage mechanism via a Rho1-independent PKC MAP kinase pathway, resulting in compensatory up-regulation of chitin synthesis to confer caspofungin resistance.

Results

Genetic screening for caspofungin-resistant *C. albicans* mutants. A transposon-insertional mutant library of haploid *C. albicans* was generated using our newly developed *piggyBac* (*PB*) transposon-mediated mutagenesis technology (Gao et al., 2018; Li et al., 2020). To screen for caspofungin-resistant mutants, the library was cultured in glucose minimum medium (GMM) at 30 °C overnight, and equal volumes of diluted culture were spread onto several YPD plates to estimate the total number of mutant cells used in the screen and onto 100 YPD plates, containing 0.25 μg/ml of caspofungin. The plates were incubated at 30 °C for 4 d to allow single colonies to grow. On YPD plates, numerous colonies grew up with relatively even sizes (Fig. 1A, top). In contrast, only a few colonies of various sizes were found on the caspofungin-containing plates (Fig. 1A, bottom), which were likely derived from mutations that had cause resistance to caspofungin (Fig. 1A, arrowheads). We picked 45 resistant colonies for further analysis. We extracted the genomic DNA from the resistant colonies and performed inverse PCR and DNA sequencing to identify the mutated genes (Gao et al., 2018; Li et al., 2020). After excluding some colonies with identical insertional mutations, we identified 22 genes, which carried a *PB* transposon insertion in either the coding region or the promoter. The identities and functions of the 22 genes are listed in Table S3. Among the 22 genes, 14 had the transposon insertion in the promoter, and 8 had the insertion in the coding region (Fig. 1B).

Both haploid and diploid *gpi7* mutants exhibit caspofungin resistance. To quantitatively assess the 22 isolated haploid mutants' resistance to caspofungin, we performed minimal inhibitory concentration (MIC) assays. Consistent with the screen results, all mutants exhibited higher MIC_{50} values than the control strain (Fig. 2A), indicating certain levels of caspofungin resistance. One of the mutants, *gpi7*:*PB*, showed the highest MIC_{50} value (Fig. 2A) and was chosen for further investigation.

We first verified the caspofungin resistance of the haploid *gpi7*:*PB* mutant by plate assays. The *gpi7*:*PB* mutant, together with its parental wild-type (WT) strain YW02, were grown in liquid YPD at 30 °C overnight. Both cultures were normalized to $OD_{600} = 1.0$ and then diluted 10 times in series from 10^{-1} to 10^{-5}. Then, 5 μl of each diluted culture were spotted onto YPD plates containing no or 0.5 μg/ml caspofungin and incubated at 30 °C for 2 d. In contrast to YW02, which showed almost no growth on the caspofungin plate, the *gpi7*:*PB* mutant exhibited robust growth (Fig. 2B), demonstrating significant resistance to caspofungin.

To ascertain that the observed caspofungin resistance is not a trait peculiar to the haploid background, we deleted both copies of *GPI7* using the *URA3* and *HIS1* selectable markers in the diploid strain BWP17 (*ura3 his1 arg4*). We then tested the *gpi*7Δ/Δ mutant's resistance to caspofungin by plate assays. We also reintegrated *URA3* and *HIS1* into BWP17 to generate the WT control strain (BWP17UH), which shares the same genetic background as the *gpi*7Δ/Δ mutant. In contrast to BWP17UH that showed significant susceptibility to caspofungin, the *gpi*7Δ/Δ mutant exhibited almost the same resistance level as the haploid *gpi7*::*PB* mutant (Fig. 2C). Reintroducing a WT *GPI7* gene into the *gpi*7Δ/Δ mutant restored the caspofungin susceptibility (Fig. 2C), confirming the loss of Gpi7 functions causing caspofungin resistance.

The *gpi7*Δ/Δ mutant has increased cell wall chitin content. It has been demonstrated that increased chitin synthesis results in -higher *C. albicans* resistance against echinocandins, including caspofungin, because higher chitin contents may offset the loss of cell wall integrity caused by echinocandin treatment (Lee et al., 2012; Walker et al., 2008). We suspected that the gained caspofungin resistance of the *gpi*7Δ/Δ mutant is attributable to increased chitin content, since a fourfold increase in a cell wall sugar glucosamine, the building block of chitin, had been observed in a *gpi*7Δ/Δ mutant (Richard et al., 2002a). To assess the chitin levels, we stained the cells of the WT (BWP17UH), the *gpi*7Δ/Δ

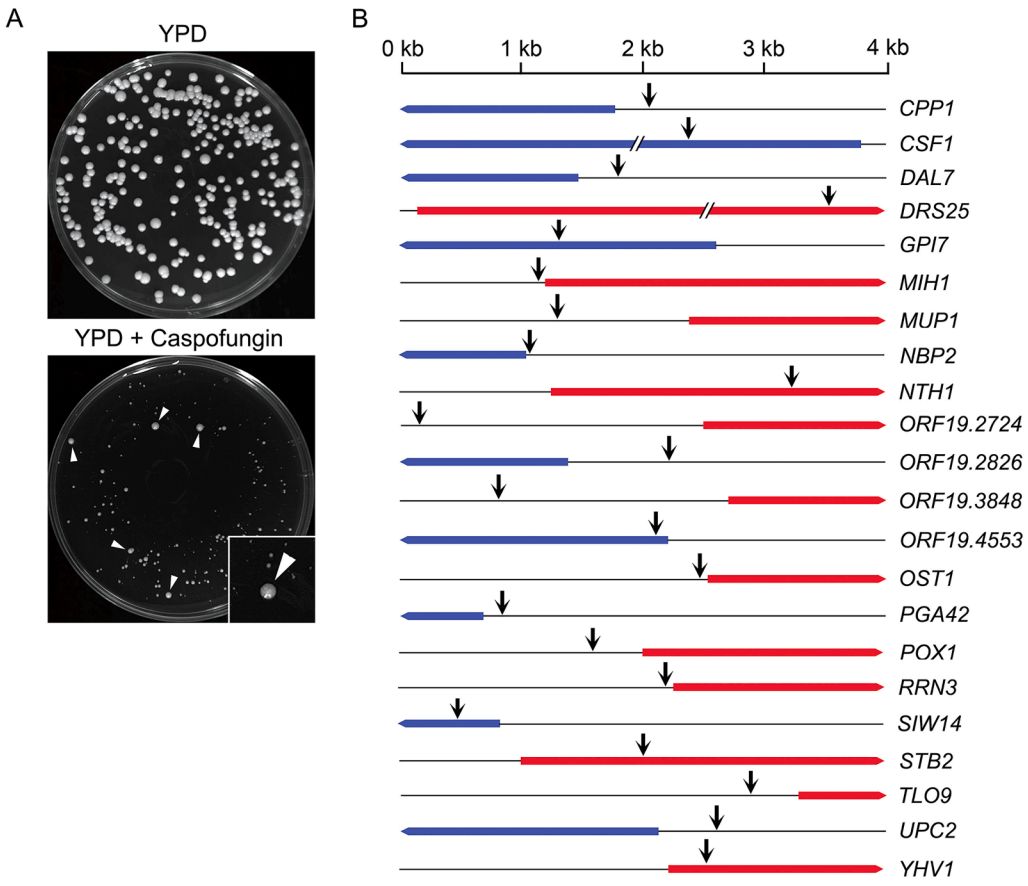

Fig. 1. A genetic screen identified 22 caspofungin-resistant haploid mutants of *C. albicans*. (A) Screening for caspofungin-resistant mutants. Approximately 30,000 *PB* transposon-mediated haploid insertional mutants were spread onto YPD plates containing 0.25 μg/ml caspofungin and incubated at 30 °C for 4 d to allow single colonies to grow. Only large colonies (arrowheads) were picked up for further analysis. To estimate the total number of mutant cells used in the screen, several YPD plates without caspofungin were also used. (B) Identification of genes mutated by *PB* transposon insertion in the caspofungin-resistant haploid mutants. Inverse PCR and DNA sequencing identified 22 mutated genes. Arrows indicate the transposon insertion site.

mutant, and the rescued strain (*gpi*7Δ/Δ:*GPI7*) with Calcofluor White (CFW). This fluorescent dye binds specifically to chitin, and its fluorescence intensity reflects the chitin level in the cell wall. All cells were incubated with the same amount of CFW simultaneously, and CFW fluorescence was captured with a fluorescence microscope. We observed much stronger fluorescence in *gpi*7Δ/Δ cells than in WT and rescued cells (Fig. 3A). Consistently, quantitative analysis confirmed that the average fluorescence intensity of *gpi*7Δ/Δ mutant cells and rescued cells is ~ 170% and 119% of that of WT cells, respectively (Fig. 3B). Together, these results confirmed the increased cell-wall chitin content in the *gpi*7Δ/Δ mutant, which could be a significant cause of the caspofungin resistance.

Deletion of *MKC1* abolishes caspofungin resistance of the *gpi*7Δ/Δ mutant. Next, we investigated the molecular mechanism by which *gpi*7Δ/Δ results in cell wall chitin content elevation. Previous studies had demonstrated that the PKC-Mkc1 MAPK pathway regulates chitin synthesis (Munro et al., 2007). This pathway enhances multiple aspects of chitin synthesis, including chitin synthase gene expression, chitin synthase enzymatic activity, and chitin levels in the cell wall (Munro et al., 2007). To determine whether the PKC-Mkc1 pathway is involved in the *gpi*7Δ/Δ-induced elevation of chitin, we examined the phosphorylation level of Mkc1, which had been shown to reflect the extent of activation of the MAP kinase pathway (de Nobel et al., 2000). Protein lysates were prepared from BWP17UH, *gpi*7Δ/Δ, and *gpi*7Δ/Δ:*GPI7* cells and subjected to immunoblotting with a phospho-Mkc1-specific antibody. We detected > 50% increase in Mkc1 phosphorylation level in *gpi*7Δ/Δ cells when compared with BWP17UH cells (Fig. 4, A and B), indicating the activation of the PKC-Mkc1 pathway in *gpi*7Δ/Δ cells. Re-integration of one WT copy of *GPI7* into *gpi*7Δ/Δ (*gpi*7Δ/Δ:*GPI7*) reduced Mkc1′s phosphorylation level significantly (Fig. 4, A and B), indicating that the loss of *GPI7* indeed promotes Mkc1 phosphorylation.

To confirm Mkc1′s role in increasing the chitin level and caspofungin resistance in *gpi*7Δ/Δ cells, we generated *mkc*1Δ/Δ in both WT and *gpi*7Δ/Δ backgrounds. We then examined the resulting strains by chitin staining and caspofungin resistance tests. Although *gpi*7Δ/Δ cells showed a much higher chitin content than *mkc*1Δ/Δ cells, combining *mkc*1Δ/Δ and *gpi*7Δ/Δ (*mkc*1Δ/Δ *gpi*7Δ/Δ cells) reduced the chitin content to a level similar to that of *mkc*1Δ/Δ cells (Fig. 4, C and D). Moreover, *gpi*7Δ/Δ cells' resistance to caspofungin was abolished by deleting *MKC1*, as *mkc*1Δ/Δ *gpi*7Δ/Δ and WT cells exhibited similar levels of caspofungin susceptibility (Fig. 4E). Taken together, these results support the idea that the PKC-Mkc1 cell wall integrity pathway mediates the caspofungin resistance of the *gpi*7Δ/Δ mutant by increasing cell wall chitin content. However, we cannot exclude the possibility that some other pathways may also be involved.

Overexpression of Rho1^{D124A} fails to suppress the caspofungin resistance of *gpi*7Δ/Δ. One major upstream regulator of the PKC-Mkc1 pathway is Rho1, which binds to and activates the protein kinase C Pkc1 to initiate the signal transduction cascade (Kamada et al., 1996; Nonaka et al., 1995). Rho1 belongs to a family of small GTP-binding proteins that cycle between GTP-bound active and GDP-bound inactive forms to fulfill their molecular-switch function (Cabib et al., 1998). To investigate whether Rho1 is also required for *gpi*7Δ/Δ-induced chitin elevation and caspofungin resistance, we overexpressed the dominant inactive Rho1^{D124A} in both WT and *gpi*7Δ/Δ strains to compare its effect on chitin contents and caspofungin resistance. Our previous study had demonstrated that overexpressing Rho1^{D124A} suppresses Rho1′s activity (Yang et al., 2018). We found that overexpressing Rho1^{D124A} neither suppressed the caspofungin resistance nor reduced the chitin level of the *gpi*7Δ/Δ mutant (Fig. 5, A-C). It also had no significant effect on WT cells. Together, these results suggest that *GPI7* deletion activates the PKC-Mkc1 cell wall integrity pathway by a mechanism independent of Rho1.

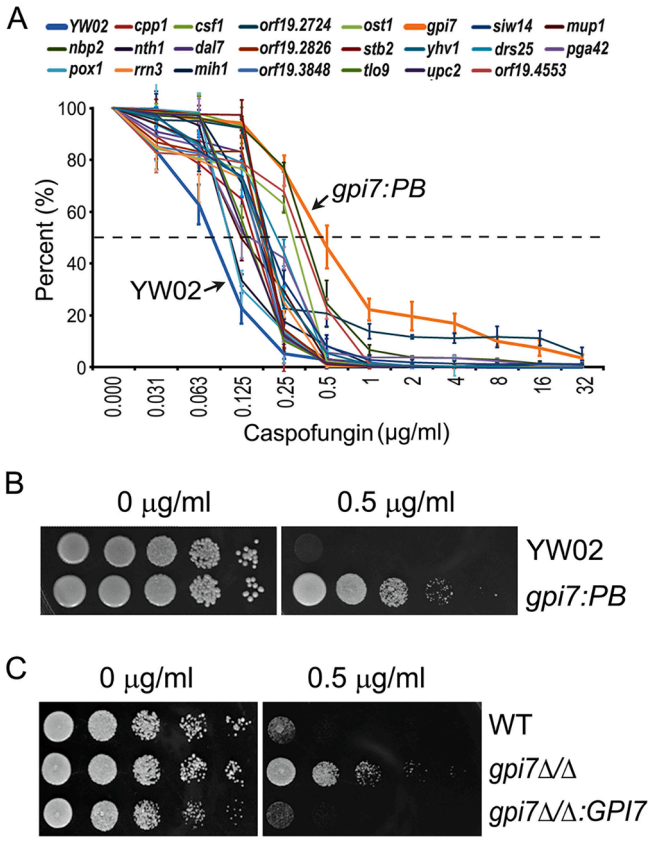

Fig. 2. Both haploid and diploid *GPI7* deletion mutants exhibit caspofungin resistance. (A) Measurement of minimal inhibitory concentration (MIC) of the isolated haploid mutants against caspofungin. Haploid insertional mutants and the WT control strain (YW02) were cultured in YPD containing 2-fold serially diluted caspofungin at 30 ℃ for 48 h. The dash line indicates 50% inhibition. For each time point, the mean of three replicates is shown, and the error bar represents standard deviation (SD). (B and C) Plate assays of caspofungin resistance of the haploid (B) and diploid (C) *gpi7* mutants. Cultures of *gpi7*:*PB* (HIM25), YW02, WT (BWP17UH), *gpi7*Δ/Δ (GZY1286) and the rescued strain *gpi7*Δ/Δ:*GPI7* (GZY1299) were normalized to $OD_{600} = 1.0$ and diluted 10 times in series, followed by spotting 5 μl of each dilution onto YPD plates containing 0 or 0.5 μg/ml of caspofungin. The plates were incubated at 30 °C for 2 d.

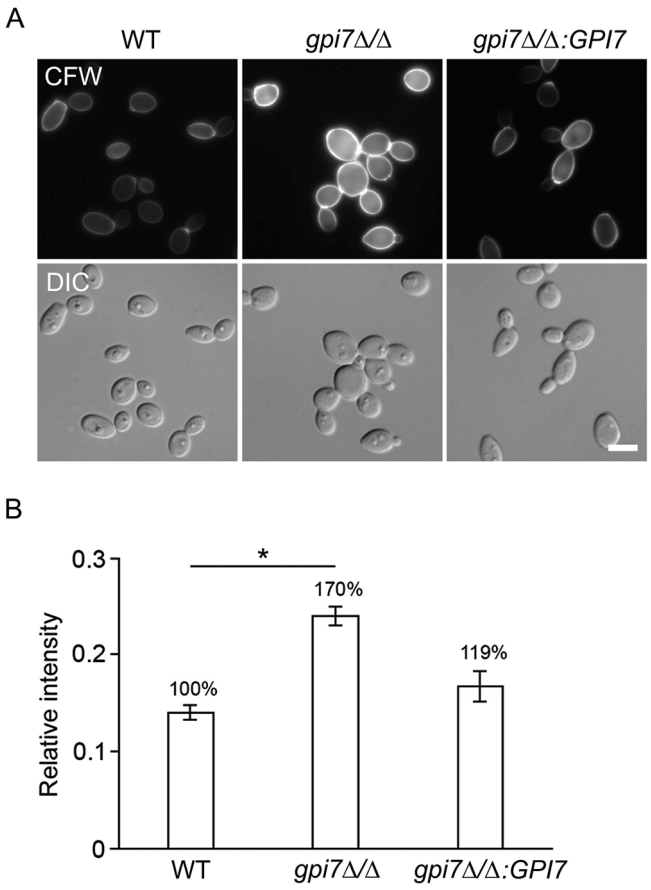

Fig. 3. The *gpi7*Δ/Δ mutant has a higher level of chitin content than WT cells. (A) Cell-wall chitin staining with CFW. Similar numbers of WT (BWP17UH), *gpi7*Δ/Δ (GZY1286), and *gpi7*Δ/Δ:*GPI7* (GZY1299) cells were incubated with CFW under the same conditions. Images for fluorescence (CFW) and differential interference contrast (DIC) were acquired using the same microscope with identical settings. Scale bar, 5 μm. (B) Quantitative analysis of fluorescence intensity of CFW on WT (BWP17UH), *gpi7*Δ/Δ, and *gpi7*Δ/Δ:*GPI7* cells. The fluorescence intensities of ≥ 80 cells from each strain were measured using Image J, and the average intensity of cells for each group was calculated for plotting. The relative fluorescence intensities of *gpi7*Δ/Δ and *gpi7*Δ/Δ:*GPI7* against that of WT are shown as percentages. The relative intensity values are the means of 3 independent measurements, and error bars represent SD. *$p < 0.05$.

Identification of genes differentially expressed in the *gpi7*Δ/Δ mutant. To further understand the molecular mechanisms underlying the *gpi7*Δ/Δ-induced caspofungin resistance, we compared the transcriptomes of the *gpi7*Δ/Δ and WT cells by RNA-Seq. Altogether, > 6000 genes were detected (Table S4), covering > 90% of the *C. albicans* genome. When $\log_2$FC > 1.5 (FC: fold change) and FDR < 0.05 (FDR: false discovery rate) were used as the screening criteria, 406 differentially expressed genes (DEGs) were identified, with 205 genes up-regulated and 201 down-regulated (Fig. 6A and Table S4). To gain insights into these DEGs' biological pathways, we performed GO (gene ontology) analysis to assign the genes into functional categories. The results showed that the significantly up-regulated genes in the *gpi7*Δ/Δ mutant were enriched with the following groups of proteins: post-translational protein targeting to the cell membrane, proteins involved in protein mannosylation and glycosylation, protein targeting to the endoplasmic reticulum, proteins having roles in glycoprotein and ergosterol biosynthetic process, and proteins associated with GPI anchor biosynthetic process (Fig. 6B). Interestingly, many down-regulated genes in the *gpi7*Δ/Δ mutant have functions in cell wall disassembly (Fig. 6C). Together, these results suggest that the deletion of *GPI7* results in compensatory cell wall synthesis and reduced cell wall disassembly activities, which could contribute to caspofungin resistance.

The *gpi7*Δ/Δ mutant exhibits attenuated virulence in mice. We examined the virulence of the *gpi7*Δ/Δ mutant in comparison with BWP17UH and *gpi7*Δ/Δ:*GPI7* strains using the mouse model of systemic infection. Approximately 1×10^6 yeast cells of each strain were injected into a mouse via the tail vein (8 mice per strain). The infected mice were monitored for survival up to 15 days (Fig. 7A). All mice injected with either the WT strain BWP17UH or the rescued strain *gpi7*Δ/Δ:*GPI7* died within 2–3 days. In contrast, mice injected with the *gpi7*Δ/Δ mutant died at a much slower rate, with > 30% remained alive on day 15 (Fig. 7A), suggesting that deleting *GPI7* attenuated the virulence of *C. albicans*. Consistently, a previous study also showed that the deletion of *GPI7* in *C. albicans* reduced its virulence and gut colonization in mice and increased sensitivity to macrophages (Richard et al., 2002b). We noted that the *gpi7*Δ/Δ mutant exhibited weak defects in hyphal growth upon serum induction, forming hyphae shorter and thicker than those of WT cells (Fig. 7B), which may partially contribute to the attenuated virulence.

Discussion

Caspofungin is a member of the echinocandin class of antifungal

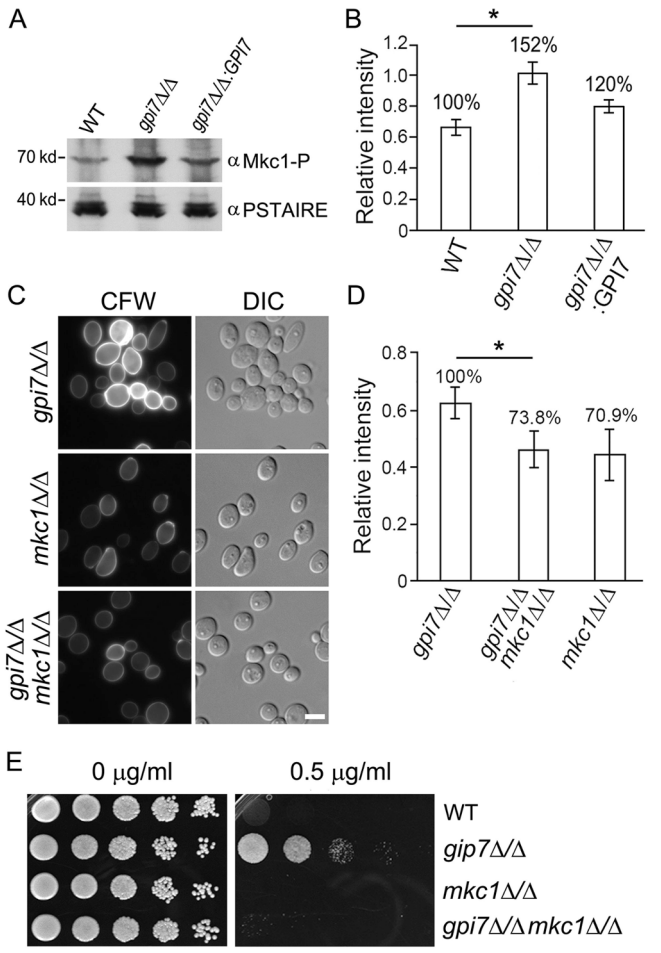

Fig. 4. *mkc*1Δ/Δ suppresses the caspofungin resistance of *gpi7*Δ/Δ. (A) Detection of Mkc1 phosphorylation level in WT (BWP17UH), *gpi7*Δ/Δ, and *gpi7*Δ/Δ:*GPI7* cells. Protein lysates were prepared and subjected to immunoblotting with anti-phosphorylated Mkc1 and anti-PSTAIRE (to detect Cdc28 as the loading control) antibodies. (B) Comparison of Mkc1 phosphorylation levels in WT, *gpi7*Δ/Δ, and *gpi7*Δ/Δ:*GPI7* cells by quantitative analysis. The densities of protein bands in Fig. 4A were measured to calculate the relative intensities of phosphorylated Mkc1 (normalized against Cdc28) for plotting. The phosphorylation levels of Mkc1 in *gpi7*Δ/Δ and *gpi7*Δ/Δ:*GPI7* relative to that in WT are shown as percentages. (C) CFW staining of cell-wall chitin in *gpi7*Δ/Δ (GZY1286), *mkc*1Δ/Δ (GZY1315), and *gpi7*Δ/Δ *mkc*1Δ/Δ (GZY1312) cells. Scale bar, 5 μm. (D) Quantitative analysis of CFW fluorescence intensity on *gpi7*Δ/Δ, *mkc*1Δ/Δ, and *gpi7*Δ/Δ *mkc*1Δ/Δ cells. The relative CFW intensities of *mkc*1Δ/Δ and *gpi7*Δ/Δ *mkc*1Δ/Δ against that of *gpi7*Δ/Δ are presented as percentages. (E) Plate assays of caspofungin resistance of WT (BWP17UH), *gpi7*Δ/Δ, *mkc*1Δ/Δ, and *gpi7*Δ/Δ *mkc*1Δ/Δ. In B and D, the relative intensity values are the means of 3 independent measurements, and error bars represent SD. $^*p < 0.05$.

compounds that noncompetitively inhibit the synthesis of β-1,3-glucan, the essential structural polysaccharide of the fungal cell wall. Caspofungin is usually fungicidal for *C. albicans*. Following its widespread use for treating and preventing fungal infection, clinical isolation of caspofungin-resistant strains is increasingly frequent. Therefore, a thorough understanding of the principal resistance mechanisms becomes critical for developing better therapeutics, improved diagnostics, and intervention strategies to overcome and prevent resistance. In this study, we isolated > 20 caspofungin-resistant mutants of *C. albicans* from a genome-wide genetic screen. We discovered that transposon-mediated inactivation of *GPI7*, a gene encoding *C. albicans* mannose-ethanolamine phosphotransferase, confers significant resistance to caspofungin. We further demonstrated that *gpi7*Δ/Δ-induced caspofungin resistance is associated with elevated cell-wall chitin content; the phenotypes can be suppressed by deleting the core component of the PKC-MAPK pathway, *MKC1*, but not by overexpressing the dominant inactive form of the PKC-MAPK pathway upstream activator *RHO1*. Together, these findings suggest that *C. albicans* cells respond to the damages caused by the deletion of *GPI7* by triggering the cell-wall salvage mechanism via a Rho1-independent PKC-MAPK pathway to activate compensatory chitin synthesis, resulting in enhanced resistance to caspofungin.

The discovery of *C. albicans* haploids and subsequent development of the haploid-based mutagenesis and screening techniques have significantly facilitated finding gene's functions via genome-wide genetic studies (Hickman et al., 2013; Mielich et al., 2018; Shapiro et al., 2018; Zeng et al., 2014). Application of these new technologies have led to the identification of novel genes implicated in biofilm formation (Seneviratne et al., 2015), azole and amphotericin B resistance (Gao et al., 2018; Truong et al., 2016), white-opaque switch (Yang et al., 2018), and antifungal mechanisms (Truong et al., 2018, 2020). Here, a transposon-mediated mutant library built using the *C. albicans* haploid again aided us in identifying > 20 new genes likely involved in caspofungin resistance (Fig. 1). Among these genes, the *gpi7*:*PB* mutant exhibited the highest resistance to caspofungin (Fig. 2A). The phenotype was further verified in the diploid background. Like the *gpi7*:*PB* mutant, the *gpi7*Δ/Δ strain showed a similar level of caspofungin resistance, which was reverted by reintroducing a WT copy of *GPI7* (Fig. 2C). Although this study has only characterized the role of *GPI7* in caspofungin resistance, existing evidence has implicated some of the other genes in drug resistance. For example, deletion of *UPC2* has been shown to decrease the resistance to fluconazole by down-regulating ergosterol biosynthesis (Silver et al., 2004). Also, deletion of the *CSF1* homologue in *Saccharomyces cerevisiae* reduced the resistance to hygromycin B (Barreto et al., 2011). Similar decreased resistance to hygromycin B had been observed in *S. cerevisiae* when the homologues of *NBP2* and *SIW14* were deleted (Dudley et al., 2005; Hirasaki et al., 2010). Finding these genes in our genetic screen suggests that they are involved in *C. albicans* resistance to caspofungin, although further investigation is required to elucidate the underlying mechanisms.

FKS1 encodes the catalytic subunit of β-1,3-glucan synthase in *C. albicans* (Mio et al., 1997), and many mutations in *FKS1* confer caspofungin resistance (Douglas et al., 1997). However, we did not isolate any *fks1* mutants from our genome-wide genetic screen. One highly possible reason is that the mutant library we used for the genetic screen did not contain *fks1* mutants capable of conferring caspofungin resistance because inactivation of *FKS1* is most likely lethal (Douglas et al., 1997). A transposon insertion within *FKS1*'s promoter or coding region in a haploid strain may either abolish the gene expression or result in an inactive, truncated Fks1. Perhaps some *fks1* mutants with transposon insertion near the C-terminal end of Fks1 may survive, but these mutants are expected to be caspofungin-susceptible. C-terminal truncated Fks1 may largely retain the intact enzyme activity, and mutations that confer caspofungin resistance are known to cluster near the N-terminal end (Park et al., 2005). Aside from *FKS1*, two nonessential genes, *GSL1* and *GSL2*, also encode putative catalytic subunits of β-1,3-glucan synthase (Mio et al., 1997). However, no evidence has demonstrated that they are also the targets of caspofungin.

Caspofungin resistance of *GPI7* mutants could be explained by Gpi7 biochemical function in GPI anchor biosynthesis. GPI anchoring is a ubiquitous mechanism for attaching proteins to the cell surface in all eukaryotic organisms. Shortly after synthesis in the endoplasmic reticulum (ER), proteins destined to be GPI-anchored will have their C-terminal signal sequence replaced by a preformed GPI anchor to target the cell surface. Most yeast GPI-anchored proteins lose part of the anchor and become covalently attached to the β-1,6-glucans of the cell wall, while a minority retains the GPI anchor in an intact form and stay at the plasma membrane (Tiede et al., 1999). For the biosynthesis of GPI anchors, phosphatidylinositol is modified by the stepwise addition of

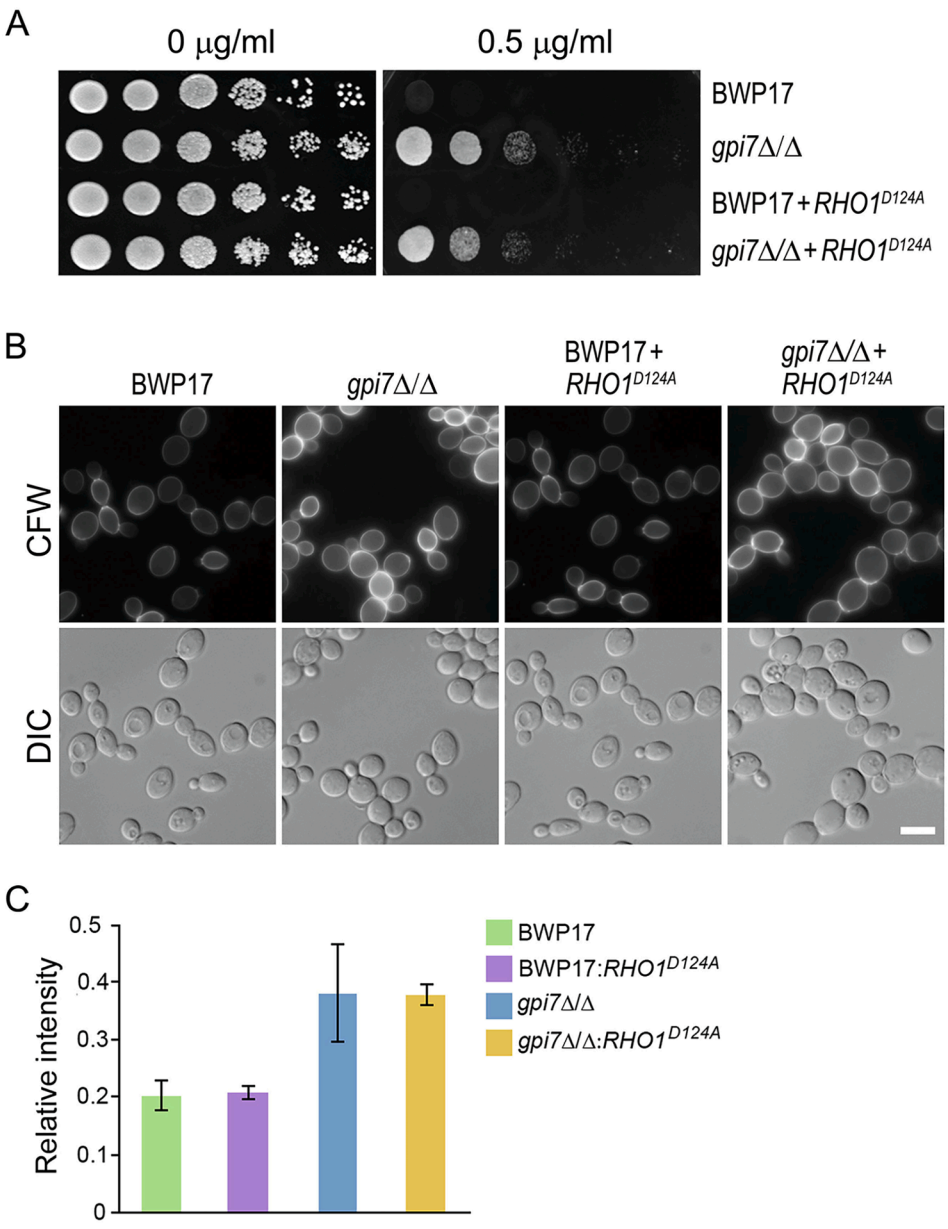

Fig. 5. Overexpression of Rho1^{D124A} fails to suppress *gpi7*Δ/Δ-induced chitin elevation and caspofungin resistance. (A) Plate assays examining the effect of overexpressed Rho1^{D124A} on caspofungin resistance. BWP17 (WT) and *gpi7*Δ/Δ cells without or with Rho1^{D124A} overexpression (GZY1294 and GZY1311, respectively) were assayed. (B) CFW staining of BWP17 and *gpi7*Δ/Δ cells with or without Rho1^{D124A} overexpression. Scale bar, 5 μm. (C) Quantitative analysis of CFW fluorescence intensity on BWP17 and *gpi7*Δ/Δ cells with or without Rho1^{D124A} overexpression. The relative intensity values are the means of 3 independent measurements, and error bars represent SD.

sugars and ethanolamine phosphate, thus forming a complete precursor which will be transferred onto newly synthesized proteins in the ER (Tiede et al., 1999). In *S. cerevisiae*, GPI anchors possess four mannose groups with a phosphoethanolamine linked on the first three groups (Tiede et al., 1999), and Gpi7 is the transferase responsible for the addition of phosphoethanolamine to the second mannose of the GPI core structure (Benachour et al., 1999; Imhof et al., 2004). Therefore, it is conceivable that some GPI-anchored proteins important for cell-wall architecture are missing in *GPI7* mutants, which impairs cell wall integrity and triggers the cell-wall salvage mechanism to activate compensatory chitin synthesis. In support of this notion, lower levels of GPI-anchored cell-wall proteins have been observed in *gpi7*Δ/Δ mutants in both *S. cerevisiae* and *C. albicans* (Richard et al., 2002a). Furthermore, we have observed the activation of the PKC-MAPK pathway as indicated by enhanced Mkc1 phosphorylation (Fig. 4A) and increased chitin content (Fig. 3) in *gpi7*Δ/Δ cells.

Our transcriptome comparison between *gpi7*Δ/Δ and WT cells further provides strong evidence for the activation of cell wall salvage mechanism in the *gpi7*Δ/Δ mutant (Fig. 6 and Table S4). The main functional groups of up-regulated genes seen in *gpi7*Δ/Δ cells belong to those involved in cell-wall biogenesis, construction, maintenance, and remodeling. For example, *GFA1* encodes the glutamine-fructose-6-phosphate amidotransferase, an enzyme involved in the first steps of the chitin synthesis pathway (Smith et al., 1996; Watzele and Tanner, 1989). *PMT1*, *PMT2*, and *PMT4*, three other up-regulated genes seen in *gpi7*Δ/Δ cells belong to a gene family encoding O-mannosyltransferases required to maintain proper cell-wall composition (Prill et al., 2005). *gpi7*Δ/Δ also caused the up-regulation of another group of genes, including *DPM1* and *DPM2*, which encode dolichol phosphate mannose synthases, the key enzymes for GPI anchor biosynthesis (Juchimiuk et al., 2015). On the other hand, the major functional groups of the down-regulated genes in *gpi7*Δ/Δ are those involved in cell-wall disassembly (Fig. 6C), such as *CSH1*, *IFD6*, and *ORF19.7214* (Table S4). *CSH1* and *IFD6* have been predicted to participate in protein hydrolysis during cell-wall deconstruction (O'Meara and O'Meara, 2021). *ORF19.7214* is an uncharacterized gene in *C. albicans*, but its homologue in *S. pombe*, Exg3, encodes a glucan 1,6-β-glucosidase involved in cell-wall decomposition (Dueñas-Santero et al., 2010). Together, these global changes of

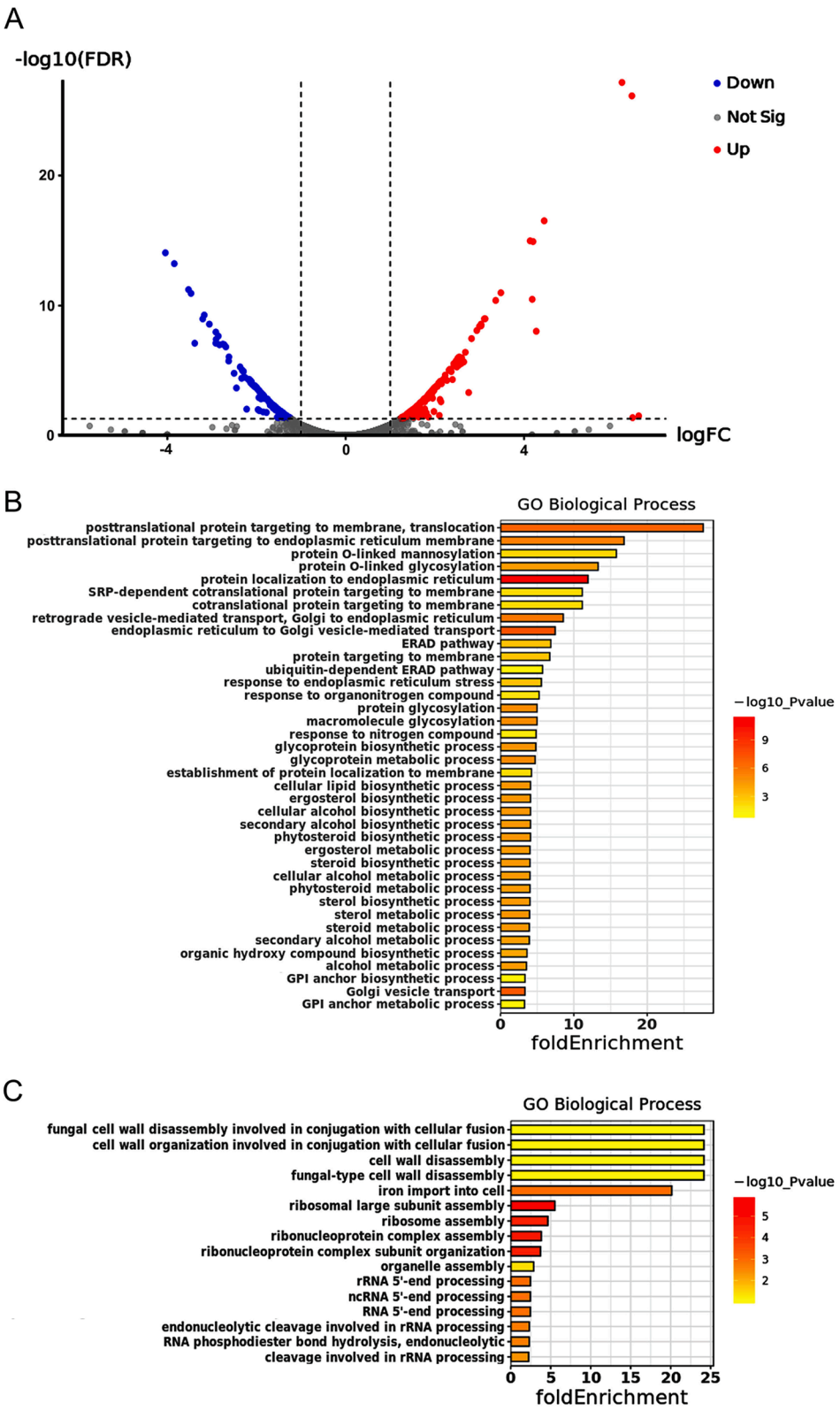

Fig. 6. RNA-Seq analysis reveals differentially expressed genes in the *gpi7*Δ/Δ mutant. (A) Volcano plot showing the distribution of differentially expressed genes. Changes with $\log_2$FC > 1.5 and FDR < 0.05 are considered significant. (B and C) Functional classification of up-regulated (B) and down-regulated (C) genes. GO analysis was conducted to determine the enrichment of genes in different biological processes.

gene expression patterns caused by the deletion of *GPI7* are in good agreement with the activation of the cell-wall salvage mechanism.

In response to cell-wall damages, yeast cells activate the cell-wall salvage mechanism, resulting in compensation characterized by a multiple-fold increase in chitin content and hyper-accumulation of glucans and mannoproteins (Popolo et al., 2001). Chitin synthesis in *C. albicans* is coordinately regulated by three signal transduction pathways, namely the PKC, HOG, and Ca^{2+} signaling pathways (Munro et al.,

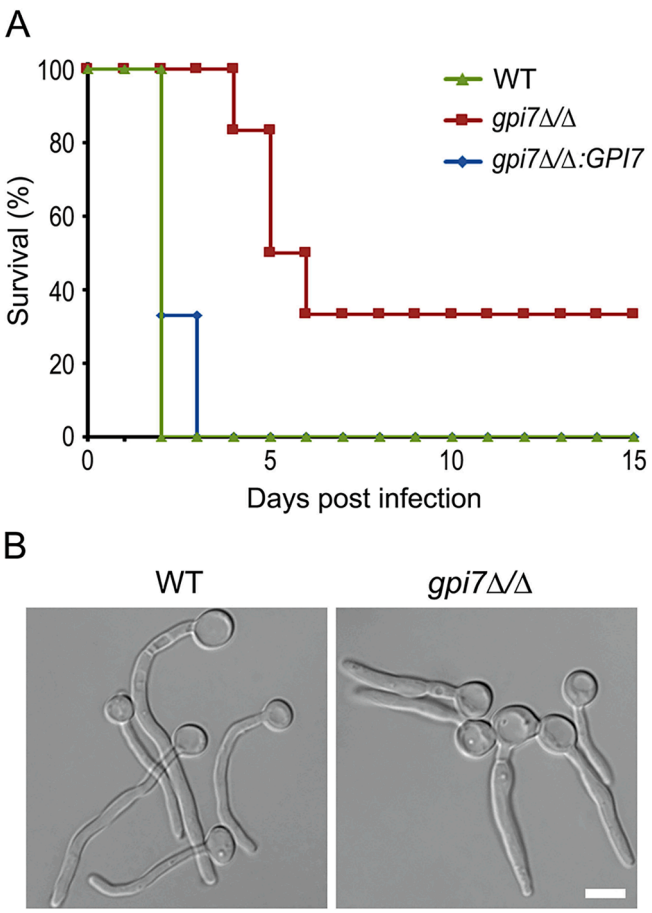

Fig. 7. Virulence of the *gpi7*Δ/Δ mutant is attenuated in the mouse model of systemic infection. (A) Virulence assay of WT (BWP17UH), *gpi7*Δ/Δ (GZY1286), and *gpi7*Δ/Δ:*GPI7* (GZY1299). 1×10^6 yeast cells of each *C. albicans* strains were injected into 8–10 weeks old BALB/c mice (n = 8 per group) via the tail vein. The infected mice were monitored for survival for 15 days. (B) Comparison of hyphal growth between WT and the *gpi7*Δ/Δ mutant. Yeast cells of WT and *gpi7*Δ/Δ were induced for hyphal growth in YPD containing 10% FBS by incubating at 37 °C for 2 h. Scale bar, 5 μm.

2007). Our studies demonstrate the involvement of the PKC pathway in enhancing chitin synthesis in the *gpi7*Δ/Δ mutant, which is evident by the increased phosphorylation of Mkc1 (Fig. 4A). Whether the other two pathways are also involved in the *gpi7*Δ/Δ-induced chitin synthesis remains uncertain. However, given the fact that abolishing the PKC pathway (by *mkc1*Δ/Δ) suppressed the elevation of chitin content in *gpi7*Δ/Δ cells largely (Fig. 4C), we reason that these two pathways may play a limited role, if any, in increasing chitin synthesis in *gpi7*Δ/Δ mutants.

How the *gpi7*Δ/Δ-induced damages on cell-wall integrity are sensed and transmitted to the PKC pathway by *C. albicans* cells remains an open question. In *S. cerevisiae*, two transmembrane proteins residing in the plasma membrane have been identified as the major cell surface sensors to activate the cell-wall integrity signaling pathway. Wsc1 is dedicated to signaling cell-wall stresses during vegetative growth (Lodder et al., 1999), while Mid2 is to signal wall stress that results from pheromone-induced morphogenesis (Rajavel et al., 1999). Both Wsc1 and Mid2 physically interact with Rom2, the guanine nucleotide exchange factor (GEF) of Rho1, to activate Rho1 and subsequently the PKC-MAPK pathway (Philip and Levin, 2001). Although the homolog of Wsc1 (but not Mid2) exists in *C. albicans*, it seems not the sensor responsible for the *gpi7*Δ/Δ-induced cell wall damages, as inactivation of Rho1 by over-expressing the dominant inactive $Rho1^{D124A}$ did not abolish the transmission of signaling to the PKC-MAPK pathway (Fig. 5). Hence, we proposed that the cell-wall damages caused by *gpi7*Δ/Δ are sensed by an unidentified sensor and transmitted via another upstream regulator of Pkc1 to the PKC-MAPK pathway, which eventually leads to the activation of the transcriptional factor Rlm1 (Jung and Levin, 1999), resulting in up-regulation of chitin synthase genes and hyperaccumulation of chitin content (Fig. 8).

The clinical relevance of our findings remains to be determined. To date, we are not aware of any reports of mutations in *GPI7* in any clinical resistance isolates. The kind of unbiased genetic screens performed in this study can reveal new mechanisms of drug resistance. We used similar approaches to identify genes that play critical roles in antifungal resistance unrelated to any known mechanisms (Gao et al., 2021, 2018). The new findings will provide directions in the future studies of whole-genome or targeted sequence analysis of clinical isolates to establish whether mutations in these newly discovered genes are responsible for resistance.

The caspofungin resistance of the *gpi7* mutant comes with a fitness cost, as shown by its reduced virulence in mice. In many studies of resistant clinical isolates and experimentally evolved strains of *Candida*, it has been found that the genetic changes that lead to drug resistance often result in significant fitness loss in the absence of antifungal drugs (Hill et al., 2015; Popp et al., 2017). However, these strains can develop compensatory mechanisms for the loss of fitness. The *gip7* mutant has a fitness advantage in the presence of caspofungin, which could keep them alive in the host during antifungal treatment, buying time for mutations to occur, which may enhance their fitness and virulence.

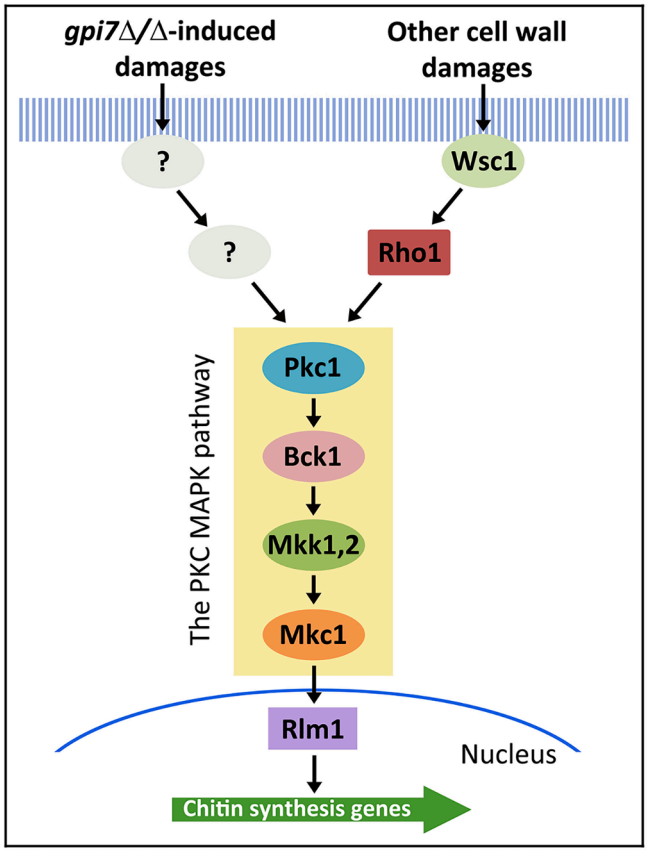

Fig. 8. A model depicting the *gpi7*Δ/Δ-induced signaling pathway. Cell-wall damages caused by *gpi7*Δ/Δ are detected by a yet unidentified sensor other than Wsc1 and transmitted by an unknown upstream activator to the PKC-MAPK signaling pathway independently of Rho1. This leads to the activation of the transcriptional factor Rlm1, which up-regulates the expression of multiple chitin synthesis genes, eventually resulting in increased chitin content in the cell wall to compensate for the loss of glucan synthesis due to caspofungin inhibition.

In summary, we have isolated > 20 haploid mutants of *C. albicans* that exhibited resistance to caspofungin from a genome-wide genetic screen. The mutant with the highest resistance has the *GPI7* gene disrupted by the transposon. *GPI7* encodes a transferase required for the addition of phosphoethanolamine to the second mannose of GPI core structure, which is an essential component of GPI-anchored cell-wall proteins. Further studies reveal that the enhanced chitin synthesis triggered by *gpi7*Δ/Δ via the PKC-MAPK pathway is the primary mechanism for caspofungin resistance. Our finding highlights a potential treatment to overcome caspofungin resistance by combining antifungals with chitin synthase inhibitors.

Methods

Strains, plasmids, and growth conditions. The construction of *C. albicans* strains and plasmids used in this study are described in Tables S1 ans S2, respectively. All haploid strains were verified for ploidy by flow cytometry analysis according to published protocols (Zeng et al., 2014). Recombinant DNA manipulations were performed according to standard methods. *E. coli* strain XL1 blue (Stratagene) was used as the host strain for recombinant plasmids and cultured in LB broth (0.5% yeast extract, 1% tryptone, and 0.5% NaCl, pH 7.0) supplemented with 100 μg/ml ampicillin. Site-directed mutagenesis followed the manual of the Quikchange multi-site-directed mutagenesis kit (Agilent Technologies). *C. albicans* cells were routinely grown at 30 °C in YPD (2% yeast extract, 1% peptone, and 2% glucose), or glucose minimal medium (GMM: 6.79 g/l yeast nitrogen base without amino acids and 2% glucose) supplemented with appropriate amino acids and other compounds (80 μg/ml uridine, 40 μg/ml arginine, 40 μg/ml histidine, and 1 mg/ml 5-Fluoroorotic acid) when necessary. For hyphal induction, overnight yeast culture was 1:20 diluted into fresh YPD medium containing 10% of fetal bovine serum (FBS) followed by incubation at 37 °C for 2 h. Solid medium plates were prepared by adding agar to 2%. Transformation of *C. albicans* with plasmids containing prototrophic markers (including the *URA3* flipper, *UFP*) was performed using the Fast Yeast Transformation Kit (G-Biosciences). All gene deletions were verified by colony PCR as described (Zeng et al., 2014), and looping out of *URA3* via FLP-mediated excision followed the previous protocol (Morschhauser et al., 1999).

Transposon-mediated insertional haploid mutant library. To generate a transposon-mediated insertional haploid mutant library, the host strain YW02 was inoculated into 5 ml YPD medium containing 50 μg/ml doxycycline and cultured at 30 °C overnight to induce the expression of *piggyBac* transposase. Cells were collected from the culture and washed twice with 25 ml of GMM. The cells were then resuspended into 50 ml of GMM and cultured at 30 °C overnight to produce a library of transposon-insertional mutants. The quality of the mutant library was verified according to the described procedures (Gao et al., 2018). The library was then aliquoted and stored at −80 °C for future use. To reveal the identity of genes mutated by transposon in isolated mutants, genomic DNA was extracted from each mutant and subjected to inverse PCR and DNA sequencing as described (Gao et al., 2018).

Minimal inhibitory concentration (MIC) assay. To perform the MIC assay, *C. albicans* cells were cultured in YPD at 30 °C overnight and then diluted with fresh YPD to yield an inoculum of 1×10^3 cells/ml. MIC assays were performed in a 96-well plate by mixing 100 μl of the inoculum of each strain with 100 μl of a series of 2-fold diluted solutions (beginning with 32 μg/ml) of caspofungin (Sigma-Aldrich). The plate was incubated at 30 °C for 48 h before measuring OD_{600} of each well by a microplate reader (Infinite 200 Pro, Tecan). The experiments were performed in triplicate, and readings for each setting were averaged and normalized against the values of drug-free wells.

Calcofluor white (CFW) staining, fluorescence microscopy and chitin content measurement. *C. albicans* cells were cultured in 5 ml of GMM at 30 °C overnight and adjusted to $OD_{600} = 1.0$. 450 μl of the culture of each strain was mixed with 50 μl of 40% formaldehyde and incubated at room temperature (RT) for 30 min. The fixed cells were washed with water twice and resuspended into the CFW solution (25 μg/ml) for incubation at RT for 1 h. The stained cells were washed with water 5 times and resuspended in the mounting medium (Vectashield). All samples were examined by using a Leica DM RXA2 microscope equipped with CoolSnap HQ2 digital camera (Roper Scientific). Images were acquired using the MetaMorph 7.5 software. For quantitative analysis of the fluorescence intensity, the acquired images were analyzed using the Image J software (https://imagej.nih.gov/ij/), and the relative intensity of a whole image was measured. Total cell numbers of the image were also counted and used to calculate the average intensity. At least 80 individual cells from > 3 images were measured and counted for each sample.

Protein extraction and Western blotting. To prepare yeast lysates, cells were harvested into 2-ml screw-cap microcentrifuge tubes by brief centrifugation to obtain the cell pellet with a volume ≤ 400 μl. The pellet was resuspended in 400 μl of ice-cold yeast lysis buffer (50 mM Tris-HCl [pH7.4], 150 mM KCl, 1% NP-40) containing the protease inhibitor cocktail (Nacalai Tesque). After adding an equal volume of acid-washed glass beads (Sigma-Aldrich), cells were broken by 5 rounds of 60-s beating at 5000 rpm in a MicroSmash MS-100 beater (TOMY Medico) with 1 min of cooling on ice between rounds. The lysed cells were then centrifuged at 16,000 rpm for 15 min at 4 °C, and supernatants were collected. The protein lysate was then mixed with an equal volume of 2 × protein loading buffer (125 mM Tris-HCl [pH 6.8], 4% SDS, 20% glycerol, 200 mM dithiothreitol, 0.02% bromophenol blue), and the mixture was boiled for 10 min before separation by 12% SDS-PAGE gel. Subsequently, proteins on the gel were transferred to a PVDF membrane (Bio-Rad Laboratories). The PVDF membrane was first incubated with 5% milk blocking solution (fat-free milk powder dissolved in phosphate-buffered saline containing 0.1% Tween-20, PBST) at RT for 1 h or at 4 °C overnight. After a brief rinse with PBST, the membrane was incubated with PBST containing a 1:2500 diluted primary antibody (rabbit polyclonal phospho-p44/42 MAPK antibody from Cell Signaling Technology or PSTAIRE antibody from Santa Cruz Biotechnology) at RT for 1 h, followed by 3 rounds of 5-min wash with PBST. The membrane was then incubated with PBST containing a 1:2500 diluted secondary antibody (HRP-linked anti-rabbit IgG antibody, Santa Cruz Biotechnology). After 3 rounds of 5-min wash with PBST, the membrane was immersed in Pierce ECL WB substrate solution (Thermo Scientific) and exposed to X-film (Fuji).

RNA extraction, sequencing libraries, and RNA-Seq. BWP17UH and *gpi7*Δ/Δ cells were cultured in YPD at 30 °C overnight before harvesting by centrifugation. Total RNA was extracted using the Trizol reagent according to the manufacturer's instructions (Sigma-Aldrich). Genomic DNA was removed using DNase I (Thermo Scientific). The total RNA was quantified using NanoDrop 1000 spectrophotometer (Thermo Scientific). RNA quality was determined by 2100 Bioanalyser (Agilent), and only high-quality RNA sample (OD260/280 = 1.8–2.2, OD260/230 ≥ 2.0, RIN ≥ 6.5, 28S:18S ≥ 1.0, >2 μg) was used to construct the sequencing library. RNA-Seq transcriptome library was prepared from 1 μg of total RNA using the TruSeq RNA sample preparation kit from Illumina. Firstly, mRNA was isolated using oligo(dT) beads to select polyA mRNA and then fragmented with the fragmentation buffer. Secondly, double-stranded cDNA was synthesized using a SuperScript double-stranded cDNA synthesis kit (Invitrogen) with random hexamer primers (Illumina). Then the synthesized cDNA was subjected to end-repair, phosphorylation, and "A" base addition according to Illumina's library construction protocol. Libraries were size-selected for cDNA target fragments of 200–300 bp on 2% Low Range Ultra Agarose followed by PCR amplification using the Phusion DNA polymerase (NEB) for 15 PCR cycles. After quantification, the paired-end RNA-Seq sequencing library was sequenced using the Illumina HiSeq xten/NovaSeq 6000 sequencer. The Illumina platform converts the sequenced image signals into textual signals and stores them as raw data in the fastq format and performs sequencing-related quality assessments on the raw

data for each sample. For data analysis, the raw paired-end reads were trimmed and quality controlled using the SeqPrep (https://github.com/jstjohn/SeqPrep) and Sickle (https://github.com/najoshi/sickle) software with default parameters. The clean reads were separately aligned to the reference genome (*C. albicans* genome assembly 21) with orientation mode using the TopHat (http://ccb.jhu.edu/software/tophat/index.shtml) software. Differential expression analysis was performed using EdgeR (https://bioconductor.org/packages/edgeR/) with bcv set to 0.2, and DEGs were selected according to $\log_2$FC > 1 and FDR < 0.05. GO analysis of the differentially expressed genes was carried out using CGD Gene Ontology Term Finder with default parameters.

Mouse model of virulence assay. BALB/c mice (8–10 weeks old) were used for this experiment. *C. albicans* strains were grown overnight in YPD medium at 30 °C and harvested by centrifugation. Cells were washed twice with phosphate-buffered saline (PBS) and resuspended in PBS at the required density. For experimental infections, each mouse was inoculated via the tail vein with 200 µl of a suspension containing 1×10^6 *C. albicans* cells in PBS. Infected mice were monitored for survival for up to 15 days. All animal experiments were conducted according to the rules and guidelines of the Agri-Food and Veterinary Authority and the National Advisory Committee for Laboratory Animal Research, Singapore. The experiments were approved by the Institutional Animal Care and Use Committee of the Biological Resource Center, Singapore (IACUC protocol 151010).

Statistical Analysis. Three biological replicates of each isolated caspofungin-resistant haploid mutants were used for the MIC assays. All experiments were repeated independently 3 times. Statistical analysis was performed using Student *t*-test. Differences were considered significant when *p*-values were < 0.05.

Data availability. The RNA-seq data are deposited under Gene Expression Omnibus accession no. GSE177483.

Declaration of Competing Interest

The authors declare that they have no known competing financial interests or personal relationships that could have appeared to influence the work reported in this paper.

Acknowledgments

We thank members of the Wang lab for helpful discussions and critical readings of the manuscript. This study was supported by OFIRG/0072/2018 and OFIRG/0055/2019 awarded to YW and BMRC042 awarded to GZ. NG acknowledges Wellcome support of a Senior Investigator (101873/Z/13/Z), Collaborative (200208/A/15/Z; 215599/Z/19/Z) and Strategic Awards (097377/Z11/Z) and the MRC Centre for Medical Mycology [MR/N006364/2].

Author contributions

GZ, experimental design, conducting experiments, data analysis, and preparation of the manuscript; XX, mouse experiments; JG, analysis of RNA-Seq data; ASD and NG, cell-wall chitin content assay; YW, experimental design, supervision of the project, writing of the manuscript, and securing funding. All authors contributed to the revision of the manuscript.

Appendix A. Supplementary data

Supplementary data to this article can be found online at https://doi.org/10.1016/j.tcsw.2021.100057.

References

Aslam, B., Wang, W., Arshad, M.I., Khurshid, M., Muzammil, S., Rasool, M.H., Nisar, M. A., Alvi, R.F., Aslam, M.A., Qamar, M.U., Salamat, M.K.F., Baloch, Z., 2018. Antibiotic resistance: a rundown of a global crisis. Infect Drug Resist. 11, 1645–1658.

Balashov, S.V., Park, S., Perlin, D.S., 2006. Assessing resistance to the echinocandin antifungal drug caspofungin in Candida albicans by profiling mutations in FKS1. Antimicrob Agents Chemother. 50 (6), 2058–2063.

Barreto, L., Canadell, D., Petrezsélyová, S., Navarrete, C., Marešová, L., Peréz-Valle, J., Herrera, R., Olier, I., Giraldo, J., Sychrová, H., Yenush, L., Ramos, J., Ariño, J., 2011. A genomewide screen for tolerance to cationic drugs reveals genes important for potassium homeostasis in Saccharomyces cerevisiae. Eukaryot Cell. 10 (9), 1241–1250.

Benachour, A., Sipos, G., Flury, I., Reggiori, F., Canivenc-Gansel, E., Vionnet, C., Conzelmann, A., Benghezal, M., 1999. Deletion of GPI7, a yeast gene required for addition of a side chain to the glycosylphosphatidylinositol (GPI) core structure, affects GPI protein transport, remodeling, and cell wall integrity. J. Biol. Chem. 274 (21), 15251–15261.

Brown, G.D., D.W. Denning, N.A. Gow, S.M. Levitz, M.G. Netea, and T.C. White. 2012. Hidden killers: human fungal infections. Sci Transl Med. 4:165rv113.

Cabib, E., Drgonová, J., Drgon, T., 1998. Role of small G proteins in yeast cell polarization and wall biosynthesis. Annu. Rev. Biochem. 67 (1), 307–333.

Chaffin, W.L., 2008. Candida albicans cell wall proteins. Microbiol. Mol. Biol. Rev. 72 (3), 495–544.

Cleveland, A.A., Farley, M.M., Harrison, L.H., Stein, B., Hollick, R., Lockhart, S.R., Magill, S.S., Derado, G., Park, B.J., Chiller, T.M., 2012. Changes in incidence and antifungal drug resistance in candidemia: results from population-based laboratory surveillance in Atlanta and Baltimore, 2008–2011. Clin. Infect. Dis. 55 (10), 1352–1361.

Cowen, L.E., Sanglard, D., Howard, S.J., Rogers, P.D., Perlin, D.S., 2015. Mechanisms of antifungal drug resistance. Cold Spring Harb. Perspect. Med. 5 (7), a019752. https://doi.org/10.1101/cshperspect.a019752.

de Nobel, H., Ruiz, C., Martin, H., Morris, W., Brul, S., Molina, M., Klis, F.M., 2000. Cell wall perturbation in yeast results in dual phosphorylation of the Slt2/Mpk1 MAP kinase and in an Slt2-mediated increase in FKS2-lacZ expression, glucanase resistance and thermotolerance. Microbiology (Reading) 146 (Pt 9), 2121–2132.

Douglas, C.M., D'Ippolito, J.A., Shei, G.J., Meinz, M., Onishi, J., Marrinan, J.A., Li, W., Abruzzo, G.K., Flattery, A., Bartizal, K., Mitchell, A., Kurtz, M.B., 1997. Identification of the FKS1 gene of Candida albicans as the essential target of 1,3-beta-D-glucan synthase inhibitors. Antimicrob. Agents Chemother. 41 (11), 2471–2479.

Dudley, A.M., Janse, D.M., Tanay, A., Shamir, R., Church, G.M., 2005. A global view of pleiotropy and phenotypically derived gene function in yeast. Mol. Syst. Biol. 1 (2005), 0001.

Dueñas-Santero, E., Martín-Cuadrado, A.B., Fontaine, T., Latgé, J.-P., del Rey, F., Vázquez de Aldana, C., 2010. Characterization of glycoside hydrolase family 5 proteins in Schizosaccharomyces pombe. Eukaryot Cell. 9 (11), 1650–1660.

Fairlamb, A.H., Gow, N.A., Matthews, K.R., Waters, A.P., 2016. Drug resistance in eukaryotic microorganisms. Nat. Microbiol. 1, 16092.

Gao, J., Wang, H., Li, Z., Wong, A.H., Wang, Y.Z., Guo, Y., Lin, X., Zeng, G., Liu, H., Wang, Y., Wang, J., 2018. Candida albicans gains azole resistance by altering sphingolipid composition. Nat. Commun. 9, 4495.

Gao, J., Chow, E.W.L., Wang, H., Xu, X., Cai, C., Song, Y., Wang, J., Wang, Y., 2021. LncRNA DINOR is a virulence factor and global regulator of stress responses in Candida auris. Nat. Microbiol.

Gizińska, M., Pytlak, W., Lis, M., Gad, B., Staniszewska, M., 2019. New trends in the search for alternative antifungal therapies. Pediatr Med. Rodz. 15 (1), 12–16.

Gow, N.A.R., Latge, J.P., Munro, C.A., 2017. The fungal cell wall: structure, biosynthesis, and function. Microbiol. Spectr. 5.

Hallen-Adams, H.E., Suhr, M.J., 2017. Fungi in the healthy human gastrointestinal tract. Virulence 8 (3), 352–358.

Hickman, M.A., Zeng, G., Forche, A., Hirakawa, M.P., Abbey, D., Harrison, B.D., Wang, Y.-M., Su, C.-H., Bennett, R.J., Wang, Y., Berman, J., 2013. The 'obligate diploid' Candida albicans forms mating-competent haploids. Nature. 494 (7435), 55–59.

Hill, J., O'Meara, T., Cowen, L., 2015. Fitness trade-offs associated with the evolution of resistance to antifungal drug combinations. Cell Rep. 10 (5), 809–819.

Hirasaki, M., Nakamura, F., Yamagishi, K., Numamoto, M., Shimada, Y., Uehashi, K., Muta, S., Sugiyama, M., Kaneko, Y., Kuhara, S., Harashima, S., 2010. Deciphering cellular functions of protein phosphatases by comparison of gene expression profiles in Saccharomyces cerevisiae. J. Biosci. Bioeng. 109 (5), 433–441.

Imhof, I., Flury, I., Vionnet, C., Roubaty, C., Egger, D., Conzelmann, A., 2004. Glycosylphosphatidylinositol (GPI) proteins of Saccharomyces cerevisiae contain ethanolamine phosphate groups on the alpha1,4-linked mannose of the GPI anchor. J. Biol. Chem. 279, 19614–19627.

Imtiaz, T., Lee, K.K., Munro, C.A., MacCallum, D.M., Shankland, G.S., Johnson, E.M., MacGregor, M.S., Bal, A.M., 2012. Echinocandin resistance due to simultaneous FKS mutation and increased cell wall chitin in a Candida albicans bloodstream isolate following brief exposure to caspofungin. J. Med. Microbiol. 61, 1330–1334.

Juchimiuk, M., Kruszewska, J., Palamarczyk, G., 2015. Dolichol phosphate mannose synthase from the pathogenic yeast Candida albicans is a multimeric enzyme. Biochim. Biophys. Acta 1850 (11), 2265–2275.

Jung, U.S., Levin, D.E., 1999. Genome-wide analysis of gene expression regulated by the yeast cell wall integrity signalling pathway. Mol. Microbiol. 34 (5), 1049–1057.

Kamada, Y., Qadota, H., Python, C.P., Anraku, Y., Ohya, Y., Levin, D.E., 1996. Activation of yeast protein kinase C by Rho1 GTPase. J. Biol. Chem. 271 (16), 9193–9196.

Kapteyn, J.C., Hoyer, L.L., Hecht, J.E., Müller, W.H., Andel, A., Verkleij, A.J., Makarow, M., Van Den Ende, H., Klis, F.M., 2000. The cell wall architecture of Candida albicans wild-type cells and cell wall-defective mutants. Mol. Microbiol. 35 (3), 601–611.
Klis, F.M., Mol, P., Hellingwerf, K., Brul, S., 2002. Dynamics of cell wall structure in Saccharomyces cerevisiae. FEMS Microbiol. Rev. 26 (3), 239–256.
Klis, F.M., Boorsma, A., De Groot, P.W.J., 2006. Cell wall construction in Saccharomyces cerevisiae. Yeast 23 (3), 185–202.
Lee, K.K., MacCallum, D.M., Jacobsen, M.D., Walker, L.A., Odds, F.C., Gow, N.A.R., Munro, C.A., 2012. Elevated cell wall chitin in Candida albicans confers echinocandin resistance in vivo. Antimicrob. Agents Chemother. 56 (1), 208–217.
Lee, K.K., Kubo, K., Abdelaziz, J.A., Cunningham, I., de Silva Dantas, A., Chen, X., Okada, H., Ohya, Y., Gow, N.A.R., 2018. Yeast species-specific, differential inhibition of beta-1,3-glucan synthesis by poacic acid and caspofungin. Cell Surf. 3, 12–25.
Lenardon, M.D., Sood, P., Dorfmueller, H.C., Brown, A.J.P., Gow, N.A.R., 2020. Scalar nanostructure of the Candida albicans cell wall; a molecular, cellular and ultrastructural analysis and interpretation. Cell Surf. 6, 100047.
Li, Z., Wang, H., Cai, C., Wong, A.-H., Wang, J., Gao, J., Wang, Y., 2020. Genome-wide piggyBac transposon-based mutagenesis and quantitative insertion-site analysis in haploid Candida species. Nat. Protoc. 15 (8), 2705–2727.
Lodder, A.L., T.K. Lee, and R. Ballester. 1999. Characterization of the Wsc1 protein, a putative receptor in the stress response of Saccharomyces cerevisiae. Genetics. 152: 1487-1499.
Mielich, K., E. Shtifman-Segal, J.C. Golz, G. Zeng, Y. Wang, J. Berman, and R. Kunze. 2018. Maize Transposable Elements Ac/Ds as Insertion Mutagenesis Tools in Candida albicans. G3 (Bethesda). 8:1139-1145.
Mio, T., Adachi-Shimizu, M., Tachibana, Y., Tabuchi, H., Inoue, S.B., Yabe, T., Yamada-Okabe, T., Arisawa, M., Watanabe, T., Yamada-Okabe, H., 1997. Cloning of the Candida albicans homolog of Saccharomyces cerevisiae GSC1/FKS1 and its involvement in beta-1,3-glucan synthesis. J. Bacteriol. 179 (13), 4096–4105.
Morschhauser, J., Michel, S., Staib, P., 1999. Sequential gene disruption in Candida albicans by FLP-mediated site-specific recombination. Mol. Microbiol. 32 (3), 547–556.
Munro, C.A., Selvaggini, S., de Bruijn, I., Walker, L., Lenardon, M.D., Gerssen, B., Milne, S., Brown, A.J.P., Gow, N.A.R., 2007. The PKC, HOG and Ca2+ signalling pathways co-ordinately regulate chitin synthesis in Candida albicans. Mol. Microbiol. 63 (5), 1399–1413.
Niimi, K., Maki, K., Ikeda, F., Holmes, A.R., Lamping, E., Niimi, M., Monk, B.C., Cannon, R.D., 2006. Overexpression of Candida albicans CDR1, CDR2, or MDR1 does not produce significant changes in echinocandin susceptibility. Antimicrob. Agents Chemother. 50 (4), 1148–1155.
Nonaka, H., Tanaka, K., Hirano, H., Fujiwara, T., Kohno, H., Umikawa, M., Mino, A., Takai, Y., 1995. A downstream target of RHO1 small GTP-binding protein is PKC1, a homolog of protein kinase C, which leads to activation of the MAP kinase cascade in Saccharomyces cerevisiae. EMBO J. 14 (23), 5931–5938.
O'Meara, T.R., O'Meara, M.J., 2021. DeORFanizing Candida albicans Genes using Coexpression. mSphere 6 (1). https://doi.org/10.1128/mSphere.01245-20.
Odds, F.C., Brown, A.J.P., Gow, N.A.R., 2003. Antifungal agents: mechanisms of action. Trends Microbiol. 11 (6), 272–279.
Park, S., Kelly, R., Kahn, J.N., Robles, J., Hsu, M.-J., Register, E., Li, W., Vyas, V., Fan, H., Abruzzo, G., Flattery, A., Gill, C., Chrebet, G., Parent, S.A., Kurtz, M., Teppler, H., Douglas, C.M., Perlin, D.S., 2005. Specific substitutions in the echinocandin target Fks1p account for reduced susceptibility of rare laboratory and clinical Candida sp. isolates. Antimicrob. Agents Chemother. 49 (8), 3264–3273.
Pfaller, M.A., Diekema, D.J., 2007. Epidemiology of invasive candidiasis: a persistent public health problem. Clin. Microbiol. Rev. 20 (1), 133–163.
Philip, B., Levin, D.E., 2001. Wsc1 and Mid2 are cell surface sensors for cell wall integrity signaling that act through Rom2, a guanine nucleotide exchange factor for Rho1. Mol. Cell Biol. 21 (1), 271–280.
Popolo, L., Gualtieri, T., Ragni, E., 2001. The yeast cell-wall salvage pathway. Med Mycol. 39 (1), 111–121.
Popp, C., Hampe, I.A.I., Hertlein, T., Ohlsen, K., Rogers, P.D., Morschhäuser, J., 2017. Competitive fitness of fluconazole-resistant clinical Candida albicans Strains. Antimicrob. Agents Chemother. 61 (7) https://doi.org/10.1128/AAC.00584-17.
Prill, S.K., Klinkert, B., Timpel, C., Gale, C.A., Schroppel, K., Ernst, J.F., 2005. PMT family of Candida albicans: five protein mannosyltransferase isoforms affect growth, morphogenesis and antifungal resistance. Mol. Microbiol. 55, 546–560.
Rajavel, M., Philip, B., Buehrer, B.M., Errede, B., Levin, D.E., 1999. Mid2 is a putative sensor for cell integrity signaling in Saccharomyces cerevisiae. Mol. Cell Biol. 19 (6), 3969–3976.
Revie, N.M., Iyer, K.R., Robbins, N., Cowen, L.E., 2018. Antifungal drug resistance: evolution, mechanisms and impact. Curr. Opin. Microbiol. 45, 70–76.
Richard, M., de Groot, P., Courtin, O., Poulain, D., Klis, F., Gaillardin, C., 2002a. GPI7 affects cell-wall protein anchorage in Saccharomyces cerevisiae and Candida albicans. Microbiology (Reading) 148, 2125–2133.
Richard, M., Ibata-Ombetta, S., Dromer, F., Bordon-Pallier, F., Jouault, T., Gaillardin, C., 2002b. Complete glycosylphosphatidylinositol anchors are required in Candida albicans for full morphogenesis, virulence and resistance to macrophages. Mol. Microbiol. 44, 841–853.
Richard, M.L., Plaine, Arnel, 2007. Comprehensive analysis of glycosylphosphatidylinositol-anchored proteins in Candida albicans. Eukaryot Cell. 6 (2), 119–133.
Ruiz-Herrera, J., Elorza, M.V., Valentin, E., Sentandreu, R., 2006. Molecular organization of the cell wall of Candida albicans and its relation to pathogenicity. FEMS Yeast Res. 6:14-29.
Sanglard, D., 2016. Emerging threats in antifungal-resistant fungal pathogens. Front. Med. (Lausanne) 3, 11.
Seneviratne, C.J., Zeng, G., Truong, T., Sze, S., Wong, W., Samaranayake, L., Chan, F.Y., Wang, Y.M., Wang, H., Gao, J., Wang, Y., 2015. New "haploid biofilm model" unravels IRA2 as a novel regulator of Candida albicans biofilm formation. Sci. Rep. 5, 12433.
Shapiro, R.S., Chavez, A., Porter, C.B.M., Hamblin, M., Kaas, C.S., DiCarlo, J.E., Zeng, G., Xu, X., Revtovich, A.V., Kirienko, N.V., Wang, Y., Church, G.M., Collins, J.J., 2018. A CRISPR-Cas9-based gene drive platform for genetic interaction analysis in Candida albicans. Nat. Microbiol. 3 (1), 73–82.
Shepherd, M.G., 1987. Cell envelope of Candida albicans. Crit. Rev. Microbiol. 15 (1), 7–25.
Silver, P.M., Oliver, B.G., White, T.C., 2004. Role of Candida albicans transcription factor Upc2p in drug resistance and sterol metabolism. Eukaryot Cell. 3 (6), 1391–1397.
Smith, R.J., Milewski, S., Brown, A.J., Gooday, G.W., 1996. Isolation and characterization of the GFA1 gene encoding the glutamine:fructose-6-phosphate amidotransferase of Candida albicans. J. Bacteriol. 178 (8), 2320–2327.
Tiede, A., Bastisch, I., Schubert, J., Orlean, P., Schmidt, R.E., 1999. Biosynthesis of glycosylphosphatidylinositols in mammals and unicellular microbes. Biol. Chem. 380, 503–523.
Truong, T., Zeng, G., Qingsong, L., Kwang, L.T., Tong, C., Chan, F.Y., Wang, Y., Seneviratne, C.J., 2016. Comparative ploidy proteomics of Candida albicans Biofilms Unraveled the Role of the AHP1 gene in the biofilm persistence against amphotericin B. Mol. Cell Proteomics 15 (11), 3488–3500.
Truong, T., Suriyanarayanan, T., Zeng, G., Le, T.D., Liu, L., Li, J., Tong, C., Wang, Y., Seneviratne, C.J., 2018. Use of haploid model of Candida albicans to uncover mechanism of action of a novel antifungal agent. Front. Cell Infect. Microbiol. 8, 164.
Truong, T., Zeng, G., Lim, T.K., Cao, T., Pang, L.M., Lee, Y.M., Lin, Q., Wang, Y., Seneviratne, C.J., 2020. Proteomics analysis of Candida albicans dnm1 haploid mutant unraveled the association between mitochondrial fission and antifungal susceptibility. Proteomics 20 (1), 1900240.
Vandeputte, P., Ferrari, S., Coste, A.T., 2012. Antifungal resistance and new strategies to control fungal infections. Int. J. Microbiol. 2012, 1–26.
Walker, L.A., Munro, C.A., de Bruijn, I., Lenardon, M.D., McKinnon, A., Gow, N.A.R., Cormack, B.P., 2008. Stimulation of chitin synthesis rescues Candida albicans from echinocandins. PLoS Pathog. 4 (4), e1000040.
Walker, L.A., Gow, N.A.R., Munro, C.A., 2010. Fungal echinocandin resistance. Fungal Genet Biol. 47 (2), 117–126.
Walker, L.A., Gow, N.A.R., Munro, C.A., 2013. Elevated chitin content reduces the susceptibility of Candida species to caspofungin. Antimicrob. Agents Chemother. 57 (1), 146–154.
Watzele, G., Tanner, W., 1989. Cloning of the glutamine:fructose-6-phosphate amidotransferase gene from yeast. Pheromonal regulation of its transcription. J. Biol. Chem. 264, 8753–8758.
Yang, S.L., Zeng, G., Chan, F.Y., Wang, Y.M., Yang, D., Wang, Y., 2018. Sac7 and Rho1 regulate the white-to-opaque switching in Candida albicans. Sci. Rep. 8, 875.
Yang, F., Zhang, L., Wakabayashi, H., Myers, J., Jiang, Y., Cao, Y., Jimenez-Ortigosa, C., Perlin, D.S., Rustchenko, E., 2017. Tolerance to caspofungin in Candida albicans is associated with at least three distinctive mechanisms that govern expression of FKS genes and cell wall remodeling. Antimicrob. Agents Chemother. 61 (5) https://doi.org/10.1128/AAC.00071-17.
Zeng, G., Wang, Y.-M., Chan, F.Y., Wang, Y., 2014. One-step targeted gene deletion in Candida albicans haploids. Nat. Protoc. 9 (2), 464–473.